Published in final edited form as:
Cancer Res. 2009 February 1; 69(3): 1212–1220. doi:10.1158/0008-5472.CAN-08-1166.

Vasculostatin inhibits intracranial glioma growth and negatively regulates *in vivo* angiogenesis through a CD36-dependent mechanism

Balveen Kaur[1,7], **Sarah M Cork**[1], **Eric M Sandberg**[1], **Narra S Devi**[1], **Zhaobin Zhang**[1], **Philip A Klenotic**[6], **Maria Febbraio**[6], **Hyunsuk Shim**[3,4,5], **Hui Mao**[4,5], **Carol Tucker-Burden**[2], **Roy L Silverstein**[6], **Daniel J Brat**[2,4], **Jeffrey J Olson**[1,4], and **Erwin G Van Meir**[1,3,4,8]

1*Laboratory of Molecular Neuro-Oncology, Department of Neurosurgery, Emory University, School of Medicine, Winship Cancer Institute, Atlanta, GA. 30322, U.S.A.*

2*Laboratory of Molecular Neuro-Oncology, Department of Pathology, Emory University, School of Medicine, Winship Cancer Institute, Atlanta, GA. 30322, U.S.A.*

3*Laboratory of Molecular Neuro-Oncology, Department of Hematology/ Oncology, Emory University, School of Medicine, Winship Cancer Institute, Atlanta, GA. 30322, U.S.A.*

4*Laboratory of Molecular Neuro-Oncology, Winship Cancer Institute, Emory University, School of Medicine, Winship Cancer Institute, Atlanta, GA. 30322, U.S.A.*

5*Laboratory of Molecular Neuro-Oncology, Department of Radiology, Emory University, School of Medicine, Winship Cancer Institute, Atlanta, GA. 30322, U.S.A.*

6*Dept of Cell Biology, Lerner Research Institute, The Cleveland Clinic, Cleveland, Ohio*

Abstract

Angiogenesis is a critical physiological process that is appropriated during tumorigenesis. Little is known about how this process is specifically regulated in the brain. Brain Angiogenesis Inhibitor-1 (BAI1) is a primarily brain specific seven-transmembrane protein that contains five anti-angiogenic thrombospondin type-1 repeats (TSR). We recently showed that BAI1 is cleaved at a conserved proteolytic cleavage site releasing a soluble, 120 kDa anti-angiogenic factor called Vasculostatin (Vstat120). Vstat120 has been shown to inhibit *in vitro* angiogenesis and suppress subcutaneous tumor growth. Here, we examine its effect on intracranial growth of malignant gliomas and further study the mechanism of its anti-tumor effects. First, we show that expression of Vstat120 strongly suppresses the intracranial growth of malignant gliomas, even in the presence of the strong pro-angiogenic stimulus mediated by the oncoprotein Epidermal Growth Factor Receptor variant III (EGFRvIII). This tumor suppressive effect is accompanied by a decrease in vascular density in the tumors, suggesting a potent anti-angiogenic effect in the brain. Second, and consistent with this interpretation, we find that treatment with Vstat120 reduces the migration of cultured microvascular endothelial cells *in vitro* and inhibits corneal angiogenesis *in vivo*. Third, we demonstrate that these

8Corresponding Author: Erwin G Van Meir, Winship Cancer Institute, Emory University School of Medicine, 1365C Clifton Rd. NE, C5078, Atlanta, GA 30322, USA, email: evanmei@emory.edu, Phone: +1 (404) 778-5563, Fax: +1 (404) 778-5550.
7New address: Dardinger Laboratory of Neuro-oncolgy and Neurosciences, James Comprehensive Cancer Center, Department of Neurological Surgery, The Ohio State University, Columbus, Ohio, 43210, U.S.A.

Author contributions:

BK performed and coordinated experiments in collaboration with NSD, ZZ and JJO for the rodent glioma models, HS and HM for the rat brain imaging, DJB and EMS for the quantification of tumor vascular density, EMS and SMC for *in vitro* angiogenesis assays, EMS and MF for the mouse corneal experiments, PK and RLS for the GST binding experiments, SMC and CTB for analysis of Vstat120 in clones and CD36 in endothelial cells and brain sections. BK and EGVM conceived project, established collaborations, designed research, interpreted results and wrote the manuscript. All authors read the manuscript.

anti-vascular effects are critically dependent on the presence of the cell surface receptor CD36 on endothelial cells *in vitro* and *in vivo*, supporting a role of the Vstat120 TSRs in mediating these effects. These results advance the understanding of brain-specific angiogenic regulation, and suggest that Vstat120 has therapeutic potential in the treatment of brain tumors and other intra-cerebral vasculopathies.

Keywords

Brain Angiogenesis Inhibitor 1 (BAI1); Vasculostatin; brain tumor; glioma

Introduction

The process of angiogenesis is tightly regulated in normal adult tissues by maintaining a delicate balance between pro-angiogenic and anti-angiogenic factors. In neoplasia, this balance is tilted in favor of new blood-vessel development, thereby increasing its vascular supply and promoting growth and metastasis (1,2). The production of pro-angiogenic molecules, such as Vascular Endothelial Growth factor (VEGF) and IL-8 is increased, and the expression of anti-angiogenic factors, such as thrombospondin-1 (TSP-1) is reduced (3,4). Arresting angiogenesis in combination with other agents is currently being exploited as an effective new therapeutic modality for cancer (5,6). Little is known about how physiological angiogenesis is regulated in the brain and how it becomes co-opted during brain tumor development.

Gliomas are the most common primary tumor of the central nervous system. Glioblastoma multiforme (GBM), the most aggressive form of malignant astrocytoma (WHO grade IV) is characterized pathologically by a highly abnormal vasculature (7). During astrocytoma progression from low to high grade, increase in vessel density precedes malignant progression as well as an accumulation of genetic defects. The two genetic alterations that coincide with transition to WHO grade IV GBM are the loss of the *PTEN* tumor suppressor gene and the amplification of the *EGFR* proto-oncogene (8,9). Apart from gene amplification and receptor over-expression, the EGFR gene is also frequently mutated in GBM. The most common of these mutations results in a truncated ligand-independent EGFRvIII with constitutive activity (10,11). Importantly, both these events are known to increase the angiogenic phenotype of glioma cells.

BAI1 is a member of the “adhesion” subfamily of G protein coupled receptors, thought to be involved in cell-cell and cell-matrix interactions (12,13). Its expression is reduced in malignant gliomas, pulmonary adenocarcinoma, pancreatic and gastric cancers, but present in the corresponding normal tissue with by far the most abundant expression in the brain (14–16). Re-expression of BAI1 in tumor cells which have lost its expression has been shown to result in slow growing tumors with reduced vessel density, suggesting an anti-angiogenic function (17,18). We recently described Vasculostatin, a naturally occurring 120 kDa fragment (Vstat120) of BAI1 (19). We have shown that Vstat120 is released from BAI1 by proteolytic cleavage at a consensus GPS site located close to the junction with the plasma membrane. Vstat120 contains an Arginine-Glycine-Aspartate (RGD) integrin recognition motif and 5 thrombospondin type 1 repeats (TSRs); both of these domains are known to mediate anti-angiogenic functions in thrombospondins (TSPs) (20–22). However it is not clear if the five TSRs contribute to the angiostatic effect of Vstat120.

We previously showed that Vstat120 can suppress the growth of glial tumors in a subcutaneous mouse xenograft model (19). However, tumor growth as well as its response to targeted treatments is affected by its location and microenvironment (23). Despite its primarily brain-specific expression, the effect of Vstat120 on the growth of intracerebral tumors has not been

investigated (13,24). Here, we examined the effects of Vstat120 on the growth of gliomas, with various degrees of malignancy and pro-angiogenic potential, in their orthotopic environment. We have further investigated the anti-angiogenic effects of Vstat120 in a number of *in vivo* and *in vitro* angiogenesis models and established that Vstat120 binding to CD36, an endothelial cell receptor for the TSR domains of TSPs-1 and -2, is essential for its angiostatic effect. These results indicate the functional significance of the five TSRs in Vstat120.

Materials and Methods

Culture of cell lines and transfection conditions

The human glioblastoma LN229 and embryonic 293 cell lines were previously described (25). Two U87MG glioblastoma cell lines maintained independently in two laboratories were used. U87MG-D cells were provided to us by Dr. D Durden's laboratory (Emory University) and were used to derive the U87MGD-Vstat120 (clones U14 and U18) by stably transfection with an expression vector for Vstat120 (pcDNA3.1mychisVstat120). U87MG-F were obtained from Dr. F Furnari's laboratory (Ludwig Institute for Cancer Research, La Jolla, CA) and were used to generate U87ΔEGFR cells which stably express the EGFRvIII mutant form of EGFR (26). U87MGD display more aggressive *in vivo* growth than U87MGF. The U87MGF-ΔEGFR-Vstat120 (clones Δ19 and Δ22) cells were prepared by stably transfecting U87MGF-ΔEGFR parental cells with pcDNA3.1mychisVstat120. The LN229Vstat120 (clone 13) and LN229TSP1 (clone C9) cells were prepared by stably transfecting LN229 cells with expression vectors for Vstat120 (pcDNA3.1mychisVstat120) and TSP1 (pcDNATS1). Conditioned media (CM) was prepared from 80% confluent cultures grown for 48–96 hours in serum free media. 293 cells were transiently transfected with the indicated plasmids using GenePORTER transfection reagent (Gene Therapy Systems) as recommended. Serum-free CM was collected from cells after 48 hours and precipitated using 50% TCA as described (19). The primary cultures of endothelial cells (HUVECs or HDMECs) were prepared by the Emory University Dermatology Core Facility and grown as described (19).

Preparation of recombinant GST fusion proteins

Two different GST/CD36 constructs containing the CLESH domain (spanning amino acids 5–143, and 67–157) were prepared as previously described (27). The GST fusion proteins were expressed in E.coli Bl21(DE3) bacteria, induced at log phase with 3mM IPTG for 3 hrs at 37° C. The bacteria were centrifuged and resuspended in 5ml of lysis buffer (PBS, one Complete mini EDTA-free protease inhibitor cocktail tablet (#4693159, Roche), and 1 mg/ml lysozyme) and frozen overnight at −20°C. The bacterial solutions were thawed in warm water and pulse sonicated (3 × 15 seconds). Lysates were sedimented at 31,000g for 30 min, followed by successive washes with buffer 1 (25ml of PBS, 0.1% Triton X-100), and buffer 2 (50mM NaH_2PO_4, 300mM NaCl, pH 8.0), and dissolved in 5ml of denaturing buffer (8M urea, 50mM Tris-HCl, pH 8.0). After 30 min centrifugation at 30,000g to remove insoluble debris, the proteins were refolded by drop wise addition into 20ml of refolding buffer (50 mM Tris-HCl, 1mM DTT, 1 mM EDTA, pH 9.0), then dialyzed overnight in 50mM Tris pH 8.0. Recombinant proteins bound to glutathione sepharose 4B resin (GE Healthcare) were either purified by elution with 50 mM Tris-HCl, 10mM glutathione or used to pull down Vstat120 or TSP1.

Glutathione-S-transferase pull-down assay

The GST-CD36-CLESH fusion protein solutions (15ml) were pre-absorbed with 100 μl of glutathione sepharose 4B beads (GE Healthcare) for 2 h at 4°C. After two washes with cold PBS, 15ml of undiluted CM (collected after 96h in serum-free medium) from stably transfected or parental control cells was added to 100 μl of beads at 4°C overnight with constant rotation. The beads were centrifuged (100 g for 1 min) and washed twice with 5 ml of PBS. Bound proteins were eluted and solubilized in 50 μl of SDS-PAGE denaturing sample buffer.

Western blot analysis

Immunoblots were performed on cell lysates (lysed in 8M Urea, 4% SDS, in 10mM Tris (pH 7.4), from indicated cells or tissue. Protein lysates (40ug) were resolved on 7.5% SDS-PAGE and Western blots probed with rabbit anti-N-terminal BAI1 (#14399) (14), or goat anti-actin (SANTA CRUZ Biotechnology Inc.; cat# SC-1616, diluted 1:500) or anti-GST (Chemicon International, MAB3317) antibodies, followed by goat anti-rabbit (DAKO Co. Carpinteria CA; Cat # P0448) or swine anti-goat (ROCHE Molecular Biochemicals, Indianapolis, IN; cat# 605275, diluted 1:1000) secondary antibodies, and visualized by enhanced chemiluminescence (PIERCE Rockford IL).

Proliferation assays

Proliferation rates of the different Vstat120-transfected and empty vector clones was assessed by the crystal violet assay (28). Equal cell numbers (4,000) of the indicated clones were plated in a 96 well plate (n=8). The cells were fixed with 1% glutaraldehyde, and then stained with 0.5% crystal violet. After washing, the crystals were dissolved in Sorenson's buffer (0.025M sodium citrate, 0.025M citric acid in 50% ethanol) and absorbance was read at A_{590} nm.

Tumorigenicity studies

Subcutaneous tumor xenografts were performed as previously described on mice marked by tattoos for identification (19,29). To establish orthotopic brain tumor xenografts, 10^6 glioma cells were stereotactically injected into the brains of athymic nude rats as described (30). Animals were anesthetized by intraperitoneal injection of Ketamine (80mg/kg)/Xylazine (10mg/kg) mixture and then secured to a stereotactic frame. Body temperature was maintained by a heating pad. A saggital midline incision was made from 5 mm anterior to the bregma to the occiput. A 2mm drill was then used to make a burr hole 3 mm to the right and 1 mm anterior of the bregma of the skull. A 23 gauge Hamilton syringe was advanced 4.5mm deep over a period of one minute, and then retracted 0.5mm prior to injecting 5μl of tumor cell suspension over a period of two minutes. Post injection, the needle was slowly retracted over a period of one minute, the burr hole filled with sterile bone wax, the skull washed with sterile water to destroy by osmosis any cells leaked into the subgaleal space and the scalp was closed with 3-0 running vicryl stitches. Survival curves were compared using the log-rank test using SPSS statistical software (version 14.0; SPSS Inc, Chicago, IL) and a P value <0.05 considered significant. Studies followed Emory University Institutional Animal Care and Use Committee guidelines.

Magnetic resonance imaging

MRI scans were carried out on a 3T MRI scanner (Philips Intera) using a small volume coil (5-cm diameter). Anesthetized animals were placed in the coil and the head secured using foam padding to minimize possible motions. MRI contrast agent, Gadolinium diethylenetriamine-pentaacetic acid (Gd-DTPA), was administrated iv. at a dose of 0.2 mM/kg to obtain signal enhancement in the tumor. Multi-slice T1-weighted spin echo images were obtained in the coronal orientation using a repetition time of 400 ms, echo time of 14 ms and imaging matrix of 128×128 with the field of view of 50 × 50 mm^2. To match the histological analysis, a slice thickness of 2 mm was used without slice gap. Number of signal average was 3 for most of the scans. T1 weighted spin echo imaging was done before and after administration of the contrast agent for each animal using the same imaging parameters.

Histological analysis

Tumors were fixed in 10% buffered formalin followed by paraffin embedding and immunohistochemistry of tissue sections (8 μm) to visualize the endothelial cells lining the blood vessels perfusing the tumor. The number of vascular structures/mm^2 in the tumor

xenografts was quantified by counting three different 10x microscopic fields for each of 3 rats/group. The three fields were averaged in each tumor and the averages for each animal used to give the final count +/− SEM.

In vitro Transwell and scratch-wound endothelial cell migration assays

CM from HEK 293 cells transfected with Vstat120 (pcDNAecBAI1myc-his) or control vector (pcDNA3.1-LacZ, a β-galactosidase expression vector) was collected and concentrated 40x using a YM-10 filter (Amicon). For the modified Boyden chamber migration assays, indicated cells were plated in Transwell chambers (Becton Dickinson Labware # 353097) with a pore size of 8 um (50,000 cells/chamber). The cells were placed on 1% serum-containing media overnight and were then pretreated with CM (diluted at 1x in endothelial medium) for 30 min. Media containing 10% serum was used as a chemo-attractant in the bottom chamber, while CM remained in the upper chamber. After 8hrs, migrated cells were quantified by counting three 10x microscopic views/filter and the data presented as means of 3 filters. Random migration in response to medium alone was subtracted from the values. For scratch-wound migration assays, confluent HDMECs were incubated in 1% media overnight in 12-well plates, then wounded with a 10μl pipet tip and detached cells were removed by PBS washes. The cells were treated with CM at a final concentration of 1x for 30 min with or without an anti-CD36 function-blocking antibody at 10 μg/mL (FA6-152, Cell Sciences), followed by incubation in 10% serum to induce cell migration. Initial wound width was measured, and the cells were allowed to migrate for 8h, and were then fixed with 1% glutaraldehyde, stained with 0.5% crystal violet, and photographed. The experiment was repeated 2 independent times and significance determined by Student's T test.

In vivo cornea angiogenesis assays

Pellets were generated as previously described (31) by mixing sterile solutions of bFGF (Research Diagnostics, Inc) at a final concentration of 25 ng/pellet, concentrated CM (50ng total protein from CM per pellet) and sucralfate (Teva Pharmaceuticals, North Wales, PA), and then spreading the solution onto nylon mesh-3-300/50 with an approximate pore size 0.4 × 0.4 mm (Tetko, Lancaster, NY). The mixture was sealed on both sides with hydron. In this case, 7.5 ul concentrated media /100 pellets were added. Individual pellets were detached by peeling the nylon mesh, and pellets of similar size were chosen under a dissecting microscope for implantation. Mice were anesthetized as above and the eyes were topically anesthetized with 0.5% proparacaine and 2% alocril and the globes proptosed with a forceps. Pellets were implanted approximately 1 mm from the limbus. Briefly, under a dissecting microscope, a central, intrastromal linear keratotomy (approximately 0.5 mm in length) was performed with a surgical blade (Bard-Parker #15; Becton Dickinson), and using the arm of a fine forceps, a micro-pocket was created toward the limbus. Pellets were placed at the base of the pocket. Erythromycin antibiotic ointment was applied to the operated eye, both to prevent infection and to decrease irritation. Mice received Buprenex (2.5 mg/kg subcutaneously) after surgery to control for pain. Five days post implantation, mice were anesthetized and 50ul of a 2.5mg/ml solution of sterile FITC-dextran (~ MW 70,000Da, Sigma) was injected into the retro-orbital sinus. The eyes were proptosed as before, and digital images of the cornea were captured under a fluorescent dissecting microscope (Leica) and transferred to Adobe Photoshop for measurements. The maximum vessel length and the neovascularization zone (in clock hours), were used to calculate the area of neovascularization, using the formula: Area (mm^2) = 0.2 × π × VL (mm) × CH. VL = vessel length; CH = clock hours, where one clock hour = 30°of an arc.

Results

Expression of Vstat120 suppresses the growth of intracranial gliomas

Since BAI1 is predominantly expressed in the brain, we investigated the role of its proteolytic cleavage product, Vstat120, on the orthotopic growth of brain tumors. We first generated two clones (U14 and U18) stably expressing, and secreting Vstat120 in human U87MGD malignant glioma cells following transfection with an expression vector (Figure 1A). The *in vitro* proliferation rates of these cells were not altered by Vstat120 expression (Figure 1B). We confirmed that conditioned media (CM) from Vstat120 expressing cells significantly inhibited the migration of human dermal microvascular endothelial cells (HDMEC) (Figure 1C) as we previously described (19). To assess the therapeutic potential of Vstat120 expression on tumor growth in the brain, we implanted U14, U18 and parental U87MGD cells (10^6/animal) stereotactically into the brains of athymic nude rats (n=6 rats/group). Both Vstat 120 expressing clones extended the median survival of animals compared to the control parental U87MGD cells ($p<0.05$). The median survival of animals injected with control parental U87MGD glioma cells was 18 days. In contrast, the median survival of the animals injected with Vstat120 expressing clones U14 and U18 was 28 (range 24–34) & 41 (range 34–49) days, respectively (Figure 1D).

Expression of Vstat120 can suppress intracranial tumor growth even when a proangiogenic stimulus is present

Parental U87MGF malignant glioma cells are pro-angiogenic due to the loss of PTEN (32). However, they lack expression of EGFRvIII, the genetic hallmark of a large subset of GBM (10,11). This mutation confers an aggressive and highly angiogenic phenotype (26,33). To test if Vstat120 could suppress the growth of such highly aggressive gliomas, we utilized U87MGF glioma cells that stably express the EGFRvIII mutant receptor (U87ΔEGFR)(26). We then stably transfected U87ΔEGFR with a Vstat120 expression vector and selected two clones (Δ19 and Δ22) for further analyses. These cells expressed Vstat120 in both the whole cell extract and conditioned medium, and did not show any alterations in their *in vitro* proliferation rates (Figure 2A). To assess the therapeutic potential of Vstat120 expression on this highly aggressive glioma, we utilized both the mouse subcutaneous and rat orthotopic xenograft models.

Athymic *nu/nu* mice (n=6/group) injected with U87ΔEGFR cells formed large subcutaneous tumors, and mice had to be sacrificed by day 25. In contrast, mice injected with Vstat120 expressing cells Vstat120 showed significant tumor growth suppression (Figure 2B). Western blot analysis of the excised tumors revealed expression of Vstat120 *in vivo* (Supplementary Figure S1). To examine whether Vstat120 would also antagonize tumor formation in their orthotopic microenvironment we implanted 10^6 cells of U87MGF, U87ΔEGFR, Δ19, and Δ22 cells stereotactically in the brain of athymic *nu/nu* rats. Initially, the effect of Vstat120 on tumor growth, was measured non-invasively by magnetic resonance imaging (MRI) on day 14 to determine tumor growth (n=3/group). Immediately thereafter the animals were sacrificed and corresponding sections of the brains were analyzed by hematoxylin and eosin (H&E) staining. Both MRI and pathology results evidenced smaller tumors in gliomas derived from cells expressing Vstat120 (Figure 2C). Next, we examined the effect of Vstat120 expression on survival of animals with intracranial tumors (n=6 animals/group). Consistent with previous reports (26), the added expression of EGFRvIII to U87MGF cells significantly reduced the median survival of rats from 31 to 21 days ($p < 0.002$). In contrast, the median survival of rats implanted with intracranial Δ19 and Δ22 cells was 57 (34 to 114 days) and 41 (days 37 to 45) days, respectively (Figure 2D).

These results demonstrated that expression of Vstat120 significantly slowed tumor growth and increased survival ($p < 0.001$ between animals implanted with either of the Vstat120 expressing clones (Δ19, and Δ22) and the control U87ΔEGFR cells). Interestingly, among rats injected with Vstat120 expressing Δ19 cells there were three long term survivors who lived for more than 60 days after tumor cell implantation. Two of these three rats eventually died of tumor burden on days 85 and 114, and the third animal was sacrificed on day 168 and found to be tumor free. Combined, the above results demonstrate that while Vstat120 has potent inhibitory effects on glioma growth *in vivo*, both in the subcutaneous and brain microenvironments.

Measurement of vascular density in intracranial gliomas

To determine whether the reduced ability of Vstat120 expressing cells to grow *in vivo* but not *in vitro* was due to impairment in recruiting the vascular supply needed for solid tumor growth, we examined the vascular phenotype of intracranial tumors derived from U87ΔEGFR and Vstat120 clones. Immunohistochemistry for von Willebrand Factor (vWF), a vascular marker, revealed a significant reduction in the density of vascular structures in Vstat120-expressing tumors (Fig. 3A). Vessel density in brain tumor sections derived from Vstat120 expressing cells (Δ19 and Δ22) showed an average of 18 (±2.0) vessels/mm^2, while control U87ΔEGFR tumors had 32 (±1.5) vessels/mm^2 ($p<0.005$) (Fig. 3B). These data demonstrate that Vstat120 can reduce the vascular density of a very aggressive form of human brain tumor in its orthotopic microenvironment in a rat model.

Vstat120-mediated inhibition of endothelial cell migration *in vitro* requires CD36

The above data, combined with our previous demonstration that Vstat120 inhibits endothelial cell migration *in vitro* (19), suggest that Vstat120 can suppress angiogenesis by antagonizing the neovascularization response of endothelial cells. Vstat120 contains five TSRs and an integrin binding RGD motif both of which are known to impart an anti-angiogenic function to thrombospondins (13,20,21,34). The anti-angiogenic effects of TSRs found in thrombospondin-1 are mediated primarily upon binding to CD36 on endothelial cells (35). Whether TSRs in non-thrombospondin proteins can also regulate angiogenesis through CD36 is currently unknown. Therefore, we examined if interactions with CD36 may play a mechanistic role in Vstat120's angiostatic function, likely through its five TSRs (35). CD36 is known to be strongly expressed on human dermal microvascular endothelial cells (HDMECs), while very little to none is found on human umbilical vein endothelial cells (HUVECs) (36). We confirmed the differential expression of CD36 in HDMEC and HUVEC (Figure 4A). To evaluate the role played by CD36 on Vstat120 antiangiogenic effect, we compared the susceptibility of CD36 expressing HDMEC and non-expressing HUVECs to the inhibitory effects of Vstat120 in a transwell migration assay. Treatment of endothelial cells with conditioned media (CM) from 293 cells expressing Vstat120 (Figure 4B, left panel) inhibited the migration of CD36 expressing HDMECs, but had no effect on CD36 non-expressing HUVEC cell migration, potentially implicating CD36 in Vstat120 effects (Figure 4B, right panel). The effect of Vstat120 on HDMEC migration was further tested in a scratch-wound migration assay (Figure 4C). Confluent HDMECs were wounded and the extent of wound closure was measured after 8 h, at which time the cells were fixed and stained. The leading edge of cells migrated a greater distance in the control cells compared to the Vstat120-treated cells. Quantification of the distance migrated, percent wound closure and migrations speed of cells showed that Vstat120 significantly reduced the migration of HDMECs.

Next, we determined whether an anti-CD36 function-blocking antibody could abrogate the inhibitory function of Vstat120 on HDMECs in a scratch-wound migration assay (Figure 4D). Confluent HDMECs were left untreated or were treated with anti-CD36 antibody for 30 minutes prior to treatment with control or Vstat120 containing CM. Quantification of these results showed that pre-incubation of HDMECs with neutralizing anti-CD36 antibody

completely abrogated the anti-migratory effect of Vstat120. Altogether these findings suggest that Vstat120 can antagonize the migration of endothelial cells in a CD36-dependent fashion.

To further examine whether these findings were consistent with the anti-tumor and anti-vascular effects of Vstat120, it was critical to demonstrate CD36 expression in brain tumor vasculature and that Vstat120 secreting glioma cells could inhibit the function of brain-derived endothelial cells *in vitro*. Immunofluorescent staining of normal brain (human and mouse) and human glioblastoma specimens for Factor VIII and CD36 confirmed the presence of CD36 in brain and glioma vasculature (Supplementary Figure S2, available on line). Transwell assays showed that the migration of human brain micro-vascular endothelial cells (HBMEC) was blocked with CM from Vstat120 expressing U14 glioma cells *in vitro* (Figure 4D).

Vstat120 can bind to the CLESH domain of CD36

The anti-angiogenic effects of TSP-1 and -2 are mediated by their binding to CD36 on endothelial cells. This interaction is dependent upon the binding of the TSR domain(s) to a conserved region within CD36 called the CLESH domain (reviewed in (37)). Consequently, we tested the ability of Vstat120 to bind to recombinant CD36 CLESH domain peptides. GST-tagged peptides spanning amino acids 5 to 143, and 67 to 157 of CD36 were expressed and purified in *E.coli* (Figure 5 A,B). The indicated GST fusion proteins were tested for their ability to bind to TSP1. Briefly the indicated recombinant peptide bound to glutathione-sepharose beads was used to pull down TSP1 from CM of LN229 cells constitutively expressing TSP1 (clone C9). Western blot of the pulled down proteins confirmed their ability to bind to TSRs. (Figure 5C, left panel). The indicated GST fusion proteins were then tested for their ability to bind to Vstat120 in a similar pull down assay using Vstat120 from CM of LN229 glioma cells constitutively expressing Vstat120. Figure 5C shows that the GST-tagged recombinant CD36 CLESH proteins, but not GST alone, pulled down Vstat120. These results demonstrate the ability of Vstat120 to bind to CLESH domain of CD36.

Vstat120 inhibits corneal angiogenesis in a CD36-dependent fashion

To examine whether Vstat120 would also inhibit neovascularization *in vivo*, we performed corneal angiogenesis assays in mice. To further assess the involvement of CD36 in this process, we compared the effects of Vstat120 on bFGF induced corneal angiogenesis in wild type and CD36 knockout mice (38). Micropellets containing human bFGF and CM of 293 cells transfected with Vstat120 cDNA or a control vector were implanted into the mice cornea. The results show that Vstat120 can reduce the extent of bFGF-induced corneal neovascularization in wild type mice (Fig 6A). This inhibitory effect was completely abolished in CD36 knockout mice. The mean area of neovascularization in corneas with pellets containing Vstat120 CM was significantly decreased (40%, $p<0.05$) as compared to those containing control CM (Fig 6B). Altogether, these results show that CD36 expression is required for Vstat120 anti-angiogenic effects on endothelial cells both *in vitro* and *in vivo*.

Discussion

We have previously shown that the cleaved and secreted 120 kDa Vstat120 fragment of BAI1, functions as an autonomous paracrine anti-angiogenic factor (19). We now show that Vstat120 expression can prolong the life of rats bearing intracranial gliomas. This tumor suppressive effect of Vstat120 in the brain was sustained even when glioma cells were engineered to over-express EGFRvIII, an oncogenic mutant EGFR resulting in highly angiogenic invasive and aggressive tumors (26). These results highlight the potential significance of harnessing Vstat120 as a therapeutic agent for the treatment of the most malignant form of glioma in humans.

Insights into the mechanism of action of various agents is critical for their development as therapeutic agents. The mechanism of Vstat120 angiostatic effect is poorly understood (19, 39). The extracellular domain of BAI1 includes five TSRs, and an integrin binding RGD motif (13). TSRs were originally discovered in TSP-1, a naturally occurring potent inhibitor of angiogenesis. TSRs are approximately 60 amino acids in length and more than 180 different TSRs have been identified in over 70 TSR-containing proteins within the human genome (40). The latter include proteins of diverse functions such as the ADAMTS family of metalloproteases, complement factors C6, C7, C8 and C9, the F-, R-and M-Spondins, Semaphorins, Unc5, Heparin binding growth-associated molecule (HB-GAM), and BAI-1, -2 and -3. The levels of sequence identity between TSR within a single protein is as diverse as that found in other TSR-containing proteins, suggesting a complex evolutionary origin (41). The high level of heterogeneity in sequence between TSRs within and across diverse proteins suggests that they may carry-out multiple functions. Based on current knowledge, homology in function cannot be inferred, but rather needs to be tested for each individual TSR. This highlights the importance of defining the function of individual TSRs in different proteins so that structural determinants can be identified in the future that will help accelerate the design of structure-function prediction algorithms. While at least five TSR-containing proteins: TSP-1 and -2, ADAMTS-1 and -8, and BAI1/Vstat120 are potent inhibitors of angiogenesis, so far only the TSR of TSPs have been convincingly linked to the anti-angiogenic activity of that protein family. Recent structural data have suggested that TSR-containing proteins could be sub-divided into two categories based on the number and orientation of the disulfide bonds between their three anti-parallel strands and the overall positive charge of their outer shell surface (42). The first category encompasses TSP-1 and -2; BAI 1–3, and the ADAMTS proteins, while the second category comprises the F-and M-spondins, and some complement proteins. The fact that all known anti-angiogenic TSR-containing proteins belong to the first category, suggest that similarity in protein anti-angiogenic action might directly derive from homology in function of some of their TSR. Furthermore, the likely mechanistic basis of this distinction is the capacity to bind the anti-angiogenic endothelial cell receptor CD36. The studies reported here support this hypothesis, as do recent studies (RLS et al, unpublished results) demonstrating that recombinant TSR from a non-angiogenic protein, F-Spondin did not bind CD36 CLESH domains.

Purified recombinant peptides expressing three of the five TSRs in BAI1 were initially shown to inhibit angiogenesis in a rabbit corneal angiogenesis assay (13). It has remained unclear, however, whether they would serve the same function in the full length human BAI1 protein; where native conformation, post-translational modifications and physiological concentrations might define activity. Recent data also showed that the TSRs of BAI1 are responsible for the recognition and engulfment of apoptotic cells by macrophages though the ELMO/Dock180/Rac signaling axis (43). Further complicating the issue is a recent study suggesting that the angiostatic effect of BAI1 was mediated by its ability to block αvβ5 integrin receptors on endothelial cells (13,39). Since the anti-angiogenic effects of thrombospondin-1 and -2 TSRs are mediated by their binding to CD36 and subsequent activation of a signaling cascade that triggers apoptosis (35,38,44), we hypothesized that the anti-angiogenic effect of Vstat120 might equally dependent on engagement of endothelial cell CD36 by Vstat120 TSRs. Brain and skin-derived endothelial cells express CD36 (44), while umbilical cord-derived HUVEC show very little expression (36). We first demonstrated that Vstat120 inhibited bFGF-induced migration of CD36-expressing HDMEC and HBMECs, but not that of HUVECs. Second, we showed that the ability of Vstat120 to inhibit HDMEC migration was suppressed in the presence of function-blocking CD36 antibodies. Third, we showed that Vstat120 inhibited corneal neovascularization in wild type but not CD36 knockout mice. Combined, our results indicate that the inhibitory effect of Vstat120 is dependent on CD36 expression on endothelial cells both *in vitro* and *in vivo*. The anti-angiogenic effect mediated by thrombospondin-1 binding to CD36 is followed by sequential activation of $p59^{fyn}$, caspase-3 like proteases and

p38 mitogen-activated protein kinases, and leads to endothelial cell apoptosis (35,38,44). The precise signaling cascade activated by Vstat120 interaction with CD36 in endothelial cells remains to be determined, but we predict that it will likely overlap with that elicited by TSP-1 given their homology in function. If this turns out to be indeed the case, the fine structural mapping of the domains involved in TSR-CD36 interactions should facilitate identification of the critical structural requirements for binding and perhaps development of computer algorithms to predict which TSR-containing proteins will be anti-angiogenic.

The CLESH domain of CD36 (amino acids 36–120) is a critical determinant of the binding of TSP-1 and -2 TSR to endothelial cells. This domain is predicted to form part of a negatively charged loop within CD36 believed to interact with the positively charged front groove of TSRs of type 1(45,46). We demonstrated the ability of Vstat120 to bind to purified peptides containing the CLESH domain of CD36, indicating a specific interaction between Vstat120 and CD36, and functional homology with TSP-1 and -2 TSR. These studies provide the first direct evidence that non-TSP TSRs of type 1 can bind CLESH domains.

These results demonstrate the significance of the endothelial receptor, CD36 in mediating Vstat120's angiostatic effect. This is the first study showing that Vstat120 is critically dependent on the presence of CD36 to suppress the process of neovascularization both *in vitro* and *in vivo*. It remains to be determined whether Vstat120's five TSRs are sufficient either singly or in combination to mediate the full anti-angiogenic effects of Vstat120, or whether the proximal RGD sequence is required for full activity. Synthetic peptides derived from TSP-1-derived TSRs have shown efficacy in preclinical models of cancer. ABT510, one such peptide, that has shown potent anti-tumorigenic effect in preclinical models and is currently being investigated in clinical trials for safety and efficacy (47,48). Future studies are warranted to refine the minimal regions of Vstat120 necessary and sufficient to mediate its anti-tumorigenic functions. This can then be exploited for the development of novel anticancer therapeutic agents that can function alone or in combination with other agents such as oncolytic viruses (49,50). Such novel agents could be Vstat peptides or peptidomimetics or alternatively, agents that could stimulate the cleavage of endogenous BAI1 in normal brain tissue to release therapeutic doses of vasculostatin.

Supplementary Material

Refer to Web version on PubMed Central for supplementary material.

Acknowledgements

We thank all the lab members for helpful comments, Dr. Y. Nakamura for the BAI1 expression vector and Drs D Durden, F Furnari and W Cavenee for U87MG-derived glioma cells.

Financial support:

This work was supported in part by grants from the NIH (CA86335 to EGVM, HL67839 to RLS, and NS056203 to BK), the National Brain Tumor Foundation and the University Research Council of Emory University (EGVM), the American Heart Association (PAK) and the Scott Hamilton Cares Foundation (RLS) and The Alex Lemonade Stand Foundation (BK). EMS was supported by an Emory University Cottrell Postdoctoral Fellowship. SC is a graduate student in the Neuroscience program of the Emory University Graduate Division of Biological and Biomedical Sciences.

References

1. Folkman J. Tumor angiogenesis: therapeutic implications. N Engl J Med 1971;285:1182–1186. [PubMed: 4938153]
2. Wang D, Anderson JC, Gladson CL. The role of the extracellular matrix in angiogenesis in malignant glioma tumors. Brain Pathol 2005;15:318–326. [PubMed: 16389944]

3. Tenan M, Fulci G, Albertoni M, et al. Thrombospondin-1 is downregulated by anoxia and suppresses tumorigenicity of human glioblastoma cells. J Exp Med 2000;191:1789–1798. [PubMed: 10811871]
4. Desbaillets I, Diserens AC, Tribolet N, Hamou MF, Van Meir EG. Upregulation of interleukin 8 by oxygen-deprived cells in glioblastoma suggests a role in leukocyte activation, chemotaxis, and angiogenesis. J Exp Med 1997;186:1201–1212. [PubMed: 9334359]
5. Batchelor TT, Sorensen AG, di Tomaso E, et al. AZD2171, a pan-VEGF receptor tyrosine kinase inhibitor, normalizes tumor vasculature and alleviates edema in glioblastoma patients. Cancer Cell 2007;11:83–95. [PubMed: 17222792]
6. Kurozumi K, Hardcastle J, Thakur R, et al. Effect of tumor microenvironment modulation on the efficacy of oncolytic virus therapy. J Natl Cancer Inst 2007;99:1768–1781. [PubMed: 18042934]
7. Brat DJ, Castellano-Sanchez AA, Hunter SB, et al. Pseudopalisades in glioblastoma are hypoxic, express extracellular matrix proteases, and are formed by an actively migrating cell population. Cancer Res 2004;64:920–927. [PubMed: 14871821]
8. Li J, Yen C, Liaw D, et al. PTEN, a putative protein tyrosine phosphatase gene mutated in human brain, breast, and prostate cancer. Science 1997;275:1943–1947. [PubMed: 9072974]
9. Smith JS, Tachibana I, Passe SM, et al. PTEN mutation, EGFR amplification, and outcome in patients with anaplastic astrocytoma and glioblastoma multiforme. J Natl Cancer Inst 2001;93:1246–1256. [PubMed: 11504770]
10. Ekstrand AJ, Sugawa N, James CD, Collins VP. Amplified and rearranged epidermal growth factor receptor genes in human glioblastomas reveal deletions of sequences encoding portions of the N- and/or C-terminal tails. Proc Natl Acad Sci U S A 1992;89:4309–4313. [PubMed: 1584765]
11. Libermann TA, Nusbaum HR, Razon N, et al. Amplification, enhanced expression and possible rearrangement of EGF receptor gene in primary human brain tumours of glial origin. Nature 1985;313:144–147. [PubMed: 2981413]
12. Shiratsuchi T, Futamura M, Oda K, et al. Cloning and characterization of BAI-associated protein 1: a PDZ domain-containing protein that interacts with BAI1. Biochem Biophys Res Commun 1998;247:597–604. [PubMed: 9647739]
13. Nishimori H, Shiratsuchi T, Urano T, et al. A novel brain-specific p53-target gene, BAI1, containing thrombospondin type 1 repeats inhibits experimental angiogenesis. Oncogene 1997;15:2145–2150. [PubMed: 9393972]
14. Kaur B, Brat DJ, Calkins CC, Van Meir EG. Brain angiogenesis inhibitor 1 is differentially expressed in normal brain and glioblastoma independently of p53 expression. Am J Pathol 2003;162:19–27. [PubMed: 12507886]
15. Hatanaka H, Oshika Y, Abe Y, et al. Vascularization is decreased in pulmonary adenocarcinoma expressing brain-specific angiogenesis inhibitor 1 (BAI1). Int J Mol Med 2000;5:181–183. [PubMed: 10639598]
16. Fukushima Y, Oshika Y, Tsuchida T, et al. Brain-specific angiogenesis inhibitor 1 expression is inversely correlated with vascularity and distant metastasis of colorectal cancer. Int J Oncol 1998;13:967–970. [PubMed: 9772287]
17. Kudo S, Konda R, Obara W, et al. Inhibition of tumor growth through suppression of angiogenesis by brain-specific angiogenesis inhibitor 1 gene transfer in murine renal cell carcinoma. Oncol Rep 2007;18:785–791. [PubMed: 17786337]
18. Kang X, Xiao X, Harata M, et al. Antiangiogenic activity of BAI1 in vivo: implications for gene therapy of human glioblastomas. Cancer Gene Ther 2006;13:385–392. [PubMed: 16244591]
19. Kaur B, Brat DJ, Devi NS, Van Meir EG. Vasculostatin, a proteolytic fragment of brain angiogenesis inhibitor 1, is an antiangiogenic and antitumorigenic factor. Oncogene 2005;24:3632–3642. [PubMed: 15782143]
20. Maubant S, Saint-Dizier D, Boutillon M, et al. Blockade of alpha v beta3 and alpha v beta5 integrins by RGD mimetics induces anoikis and not integrin-mediated death in human endothelial cells. Blood 2006;108:3035–3044. [PubMed: 16835373]
21. Volpert OV, Zaichuk T, Zhou W, et al. Inducer-stimulated Fas targets activated endothelium for destruction by anti-angiogenic thrombospondin-1 and pigment epithelium-derived factor. Nat Med 2002;8:349–357. [PubMed: 11927940]

22. Sun X, Skorstengaard K, Mosher DF. Disulfides modulate RGD-inhibitable cell adhesive activity of thrombospondin. J Cell Biol 1992;118:693–701. [PubMed: 1379247]
23. Blouw B, Song H, Tihan T, et al. The hypoxic response of tumors is dependent on their microenvironment. Cancer Cell 2003;4:133–146. [PubMed: 12957288]
24. Mori K, Kanemura Y, Fujikawa H, et al. Brain-specific angiogenesis inhibitor 1 (BAI1) is expressed in human cerebral neuronal cells. Neurosci Res 2002;43:69–74. [PubMed: 12074842]
25. Ishii N, Maier D, Merlo A, et al. Frequent co-alterations of TP53, p16/CDKN2A, p14ARF, PTEN tumor suppressor genes in human glioma cell lines. Brain Pathol 1999;9:469–479. [PubMed: 10416987]
26. Nishikawa R, Ji XD, Harmon RC, et al. A mutant epidermal growth factor receptor common in human glioma confers enhanced tumorigenicity. Proc Natl Acad Sci U S A 1994;91:7727–7731. [PubMed: 8052651]
27. Pearce SF, Roy P, Nicholson AC, et al. Recombinant glutathione S-transferase/CD36 fusion proteins define an oxidized low density lipoprotein-binding domain. J Biol Chem 1998;273:34875–34881. [PubMed: 9857015]
28. Hudziak RM, Lewis GD, Winget M, et al. p185HER2 monoclonal antibody has antiproliferative effects in vitro and sensitizes human breast tumor cells to tumor necrosis factor. Mol Cell Biol 1989;9:1165–1172. [PubMed: 2566907]
29. Van Meir EG. Identification of nude mice in tumorigenicity assays. Int J Cancer 1997;71:310. [PubMed: 9139859]
30. Bowers G, He J, Schulz K, et al. Efficacy of adenoviral p53 delivery with SCH58500 in the intracranial 9l and RG2 models. Front Biosci 2003;8:a54–a61. [PubMed: 12700117]
31. Kenyon BM, Voest EE, Chen CC, et al. A model of angiogenesis in the mouse cornea. Invest Ophthalmol Vis Sci 1996;37:1625–1632. [PubMed: 8675406]
32. Wen S, Stolarov J, Myers MP, et al. PTEN controls tumor-induced angiogenesis. Proc Natl Acad Sci U S A 2001;98:4622–4627. [PubMed: 11274365]
33. Abe T, Terada K, Wakimoto H, et al. PTEN decreases in vivo vascularization of experimental gliomas in spite of proangiogenic stimuli. Cancer Res 2003;63:2300–2305. [PubMed: 12727853]
34. Adams JC, Lawler J. The thrombospondins. Int J Biochem Cell Biol 2004;36:961–968. [PubMed: 15094109]
35. Dawson DW, Pearce SF, Zhong R, et al. CD36 mediates the In vitro inhibitory effects of thrombospondin-1 on endothelial cells. J Cell Biol 1997;138:707–717. [PubMed: 9245797]
36. Swerlick RA, Lee KH, Wick TM, Lawley TJ. Human dermal microvascular endothelial but not human umbilical vein endothelial cells express CD36 in vivo and in vitro. J Immunol 1992;148:78–83. [PubMed: 1370173]
37. Simantov R, Silverstein RL. Cd36: a critical anti-angiogenic receptor. Front Biosci 2003;8:S874–S882. [PubMed: 12957861]
38. Jimenez B, Volpert OV, Crawford SE, et al. Signals leading to apoptosis-dependent inhibition of neovascularization by thrombospondin-1. Nat Med 2000;6:41–48. [PubMed: 10613822]
39. Koh JT, Kook H, Kee HJ, et al. Extracellular fragment of brain-specific angiogenesis inhibitor 1 suppresses endothelial cell proliferation by blocking alphavbeta5 integrin. Exp Cell Res 2004;294:172–184. [PubMed: 14980512]
40. de Fraipont F, Nicholson AC, Feige JJ, Van Meir EG. Thrombospondins and tumor angiogenesis. Trends Mol Med 2001;7:401–407. [PubMed: 11530335]
41. Nicholson AC, Malik SB, Logsdon JM Jr, Van Meir EG. Functional evolution of ADAMTS genes: evidence from analyses of phylogeny and gene organization. BMC Evol Biol 2005;5:11. [PubMed: 15693998]
42. Tan K, Duquette M, Liu JH, et al. Heparin-induced cis- and trans- dimerization modes of the thrombospondin-1 N-terminal domain. J Biol Chem. 2007
43. Park D, Tosello-Trampont AC, Elliott MR, et al. BAI1 is an engulfment receptor for apoptotic cells upstream of the ELMO/Dock180/Rac module. Nature. 2007

44. Anderson JC, Grammer JR, Wang W, et al. ABT-510, a modified type 1 repeat peptide of thrombospondin, inhibits malignant glioma growth in vivo by inhibiting angiogenesis. Cancer Biol Ther 2007;6:454–462. [PubMed: 17384534]
45. Crombie R, Silverstein RL, MacLow C, et al. Identification of a CD36-related thrombospondin 1-binding domain in HIV-1 envelope glycoprotein gp120: relationship to HIV-1-specific inhibitory factors in human saliva. J Exp Med 1998;187:25–35. [PubMed: 9419208]
46. Crombie R, Silverstein R. Lysosomal integral membrane protein II binds thrombospondin-1. Structure-function homology with the cell adhesion molecule CD36 defines a conserved recognition motif. J Biol Chem 1998;273:4855–4863. [PubMed: 9478926]
47. Rusk A, McKeegan E, Haviv F, et al. Preclinical evaluation of antiangiogenic thrombospondin-1 peptide mimetics, ABT-526 and ABT-510, in companion dogs with naturally occurring cancers. Clin Cancer Res 2006;12:7444–7455. [PubMed: 17189418]
48. Markovic SN, Suman VJ, Rao RA, et al. A phase II study of ABT-510 (thrombospondin-1 analog) for the treatment of metastatic melanoma. Am J Clin Oncol 2007;30:303–309. [PubMed: 17551310]
49. Kurozumi K, Hardcastle J, Thakur R, et al. Oncolytic HSV-1 Infection of Tumors Induces Angiogenesis and Upregulates CYR61. Mol Ther. 2008
50. Post DE, Devi NS, Li Z, et al. Cancer therapy with a replicating oncolytic adenovirus targeting the hypoxic microenvironment of tumors. Clin Cancer Res 2004;10:8603–8612. [PubMed: 15623644]

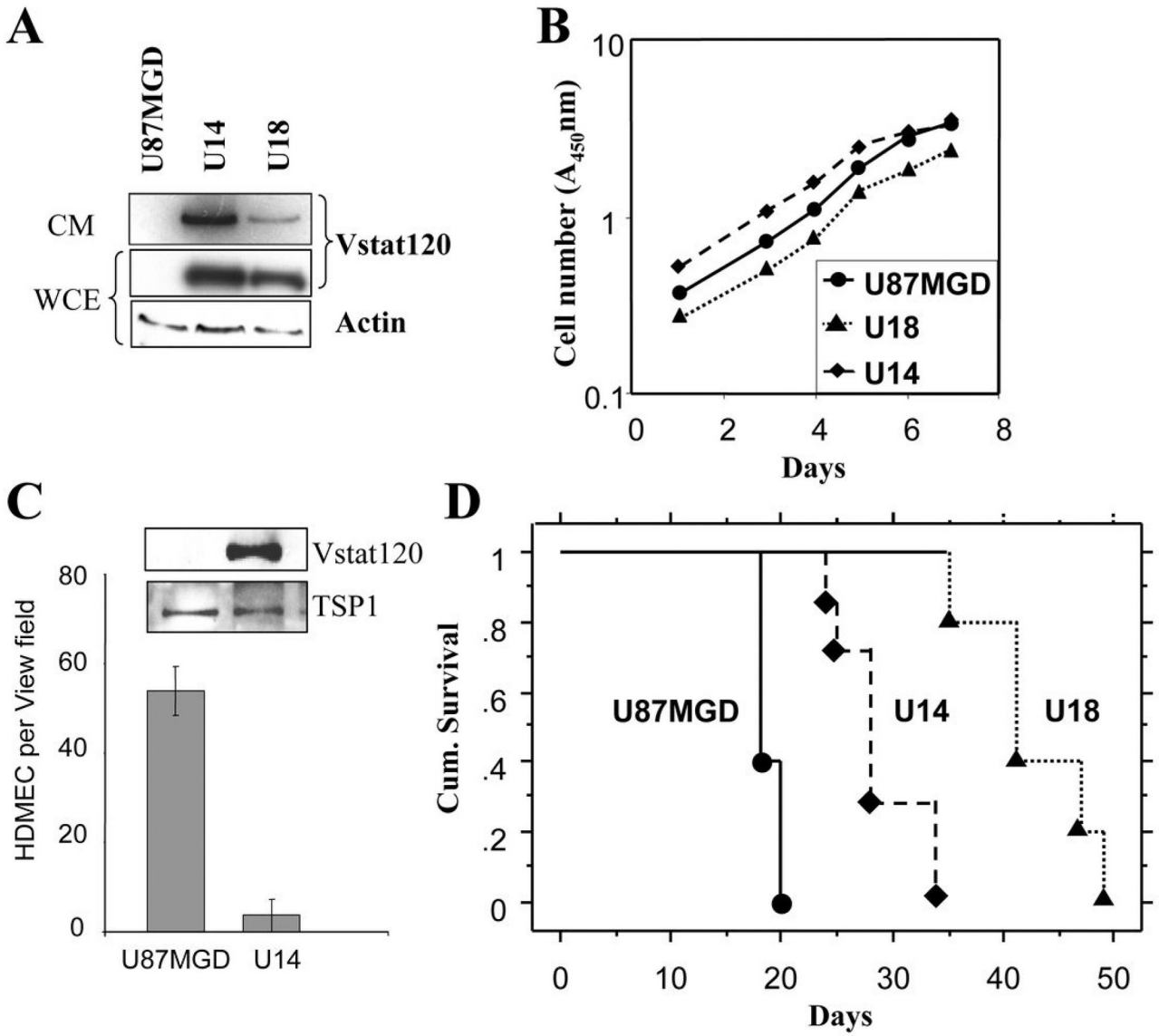

Figure 1. Expression of Vstat120 enhances survival of rats implanted with U87MGD glioma cells in the brain

A. Western blot analysis of cell lysates from U87MG parental cells, and U87MG-derived clones stably transfected with Vstat120 cDNA (U14 and U18). Note the expression of Vstat120 in the whole cell extract (WCE) and conditioned medium (CM) of the stably transfected clones. **B**. The *in vitro* proliferation rates of U87MG cells, and clones U14 and U18 was determined by the crystal violet assay. Note expression of Vstat120 did not alter the proliferation rate of the clones versus U87MG cells. **C**. CM from control U87MGD or Vstat120 expressing U14 cells were tested for their ability to inhibit the migration of HDMECs in a Transwell migration assay. The number of cells that migrated to the bottom of the chamber after 8 hrs was quantified as described in materials and methods. Random migration in response to medium alone was subtracted from the values. Expression levels of Vstat120 and thrombospondin-1 (TSP1) in the CM were assessed by Western blot. **D**. Intracranial tumorigenicity assay for U87MG and Vstat120 expressing clones, U14 and U18. 1×10^6 cells were implanted stereotactically in the brain of athymic nude rats. Survival curves of rats implanted with cells expressing Vstat120

showed a significant improvement in their survival compared to the control parental U87MG cells ($p<0.05$).

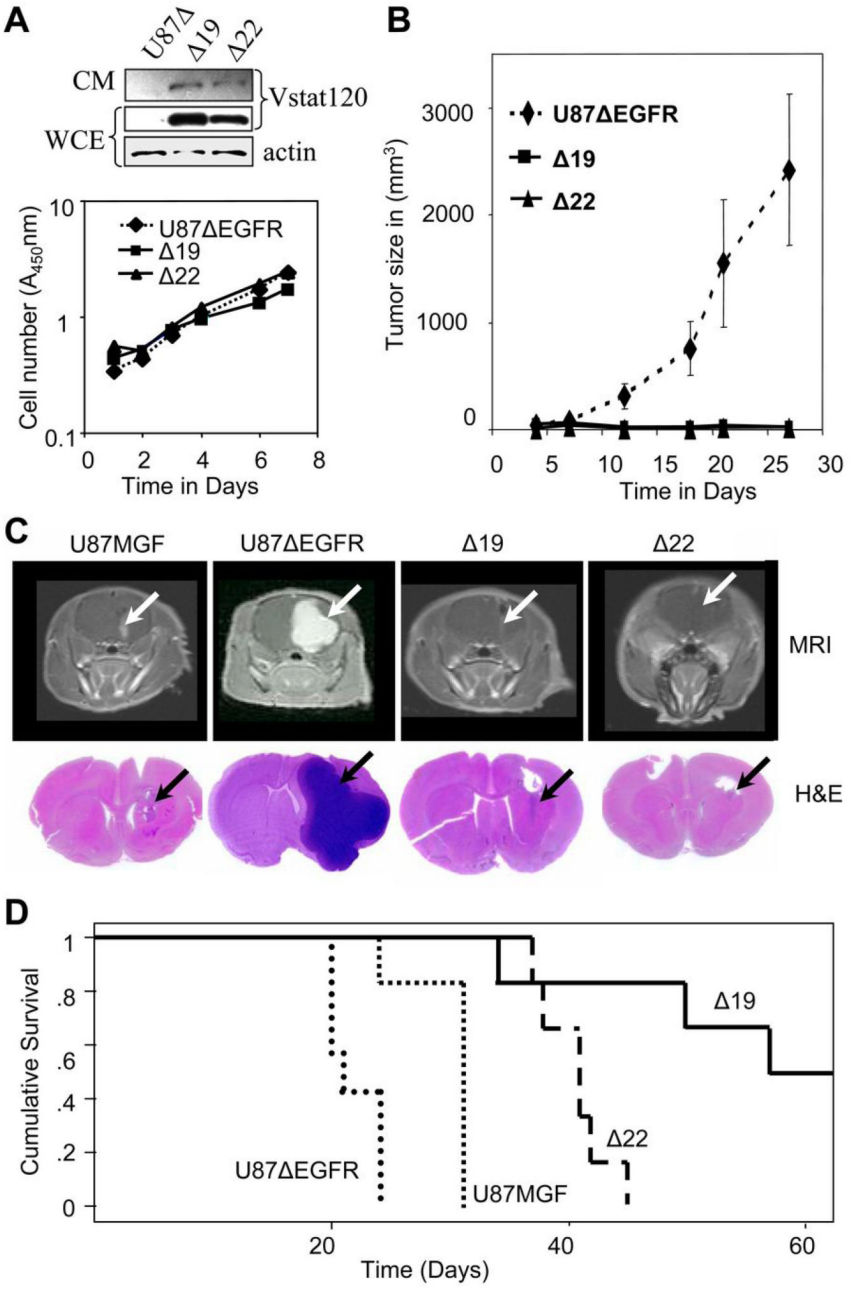

Figure 2. Vstat120 expression suppresses subcutaneous and intracranial tumor growth of U87ΔEGFR cells despite the pro-angiogenic stimulus provided by EGFRvIII

A. Characterization of U87ΔEGFR and Vstat 120 expressing clones Δ19 and Δ22. Upper Panel shows western blot analysis of whole cell extract (WCE) and conditioned medium (CM) from U87ΔEGFR cells (U87Δ) and derived clones Δ19 and Δ22, which stably express Vstat120. Lower panel shows *in vitro* proliferation rates of U87ΔEGFR cells, and Vstat120 expressing clones Δ19 and Δ22, as measured using the crystal violet assay. Expression of Vstat120 does not alter the *in vitro* proliferation rates of these cells.

B. Subcutaneous growth of U87ΔEGFR and Vstat120-expressing clones in *nu/nu* mice. U87ΔEGFR and derived clones stably expressing Vstat120 (Δ19 and Δ22) were injected

subcutaneously into mice (n=6) and the tumor volume for the indicated clones was plotted as a function of time. Note the strongly decreased tumor growth of clones expressing Vstat120.
C. Relative growth of U87MGF, U87ΔEGFR and Vstat120-expressing clones in rat brains. Upper panels show representative images of the MRI scans of individual rat brains 14 days after intracranial implantation of 10^6 tumor cells. The presence of glioma is detected through the bright areas (white arrows) of contrast enhancement from the MRI contrast agent (Gd-DTPA). Note the small tumor in U87MGF cells, large tumor in U87ΔEGFR cells and barely detectable minimal tumors in clones Δ22 and Δ19. The lower panel shows corresponding histopathological brain sections stained with H&E. Tumor growth is visible as a darkly stained area (black arrow).
D. Survival curves of rats implanted with U87MGF, U87ΔEGFR and Vstat120 expressing clones, Δ 19 and Δ22. 1×10^6 cells were implanted stereotactically in the brain of athymic *nu/nu* rats. Rats implanted with U87ΔEGFR cells had the shortest survival time due to the very angiogenic and aggressive nature of these tumors. Vstat120 expressing clones Δ19 and Δ22, showed a significant improvement in their survival compared to the U87ΔEGFR and control parental U87MGF cells ($p<0.05$).

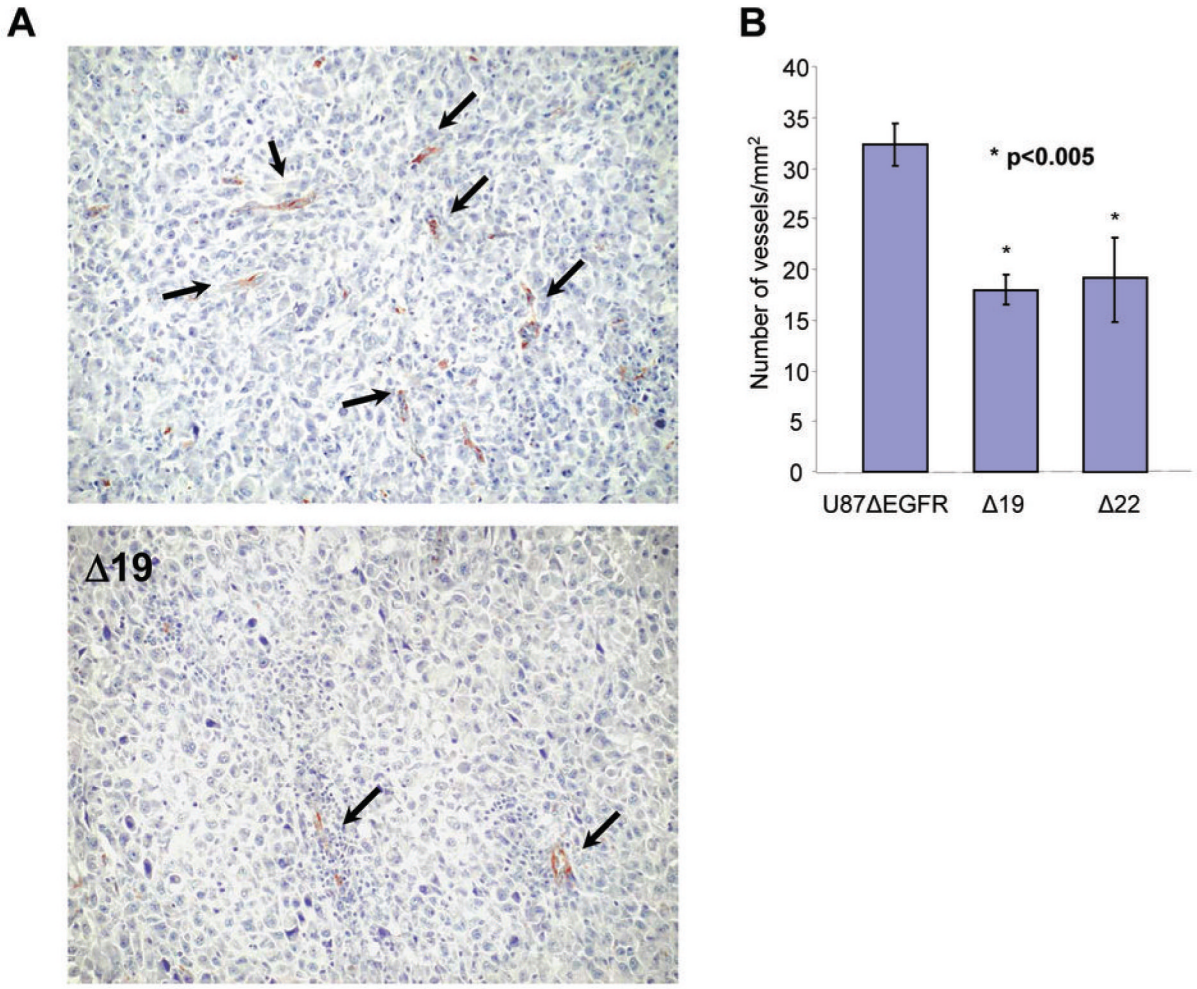

Figure 3. *In vitro* and *In vivo* Antiangiogenic effect of Vstat120 produced by glioma cells

A. Representative pictures of the immunohistochemistry for von Willebrand factor in tumor sections derived from U87ΔEGFR or Vstat120 expressing clone (Δ19) are shown. Brown staining indicates endothelial cells lining capillaries (arrows). **B**. Vessel densities in U87ΔEGFR and Vstat120 expressing clones (Δ19 and Δ22) were determined. Vstat120-expressing tumors showed significantly lower vessel density than parental tumors. Vessel densities are expressed as mean +/− SEM. * p<0.005

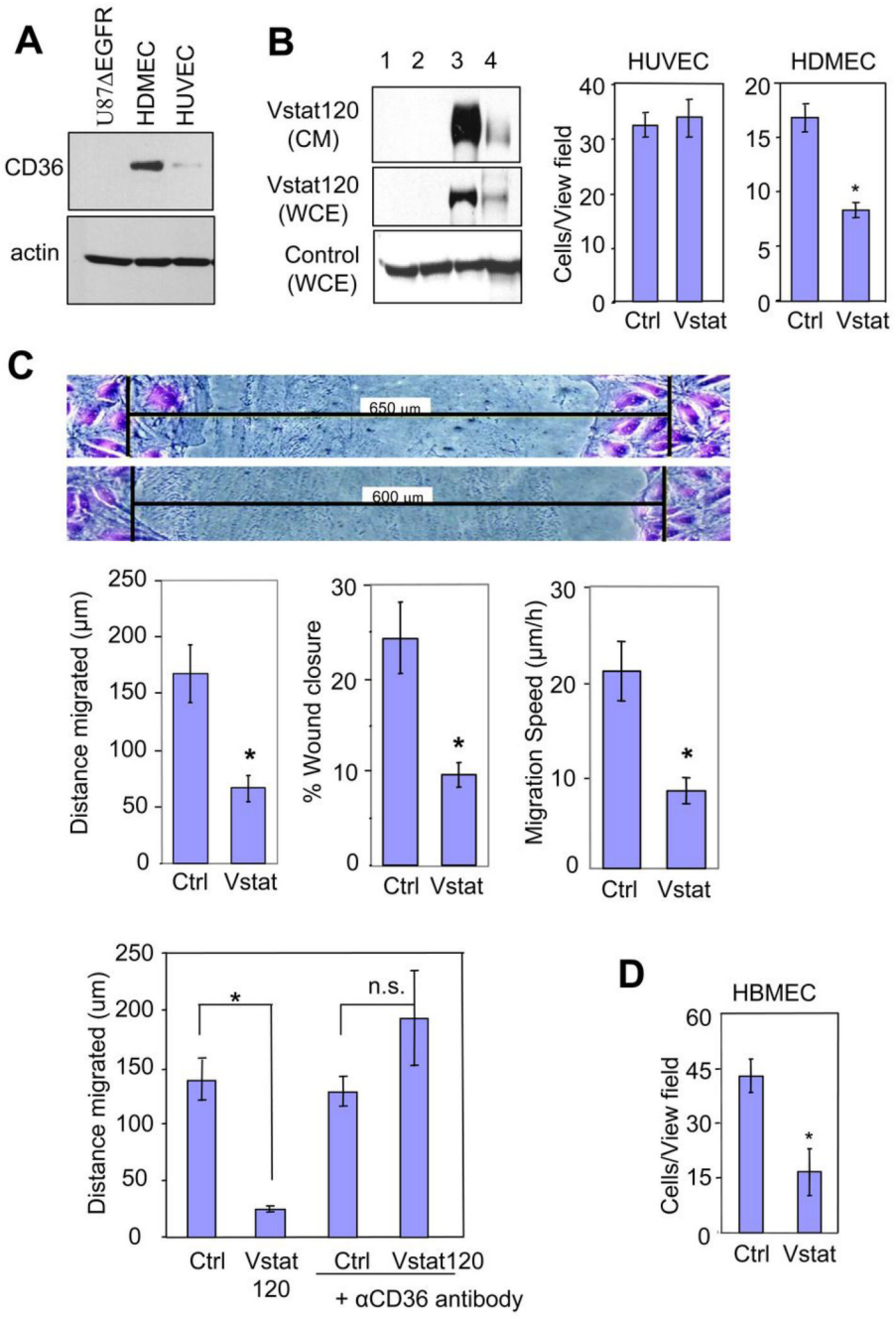

Figure 4. Vstat120 inhibits endothelial cell migration in a CD36-dependent fashion

A. Western blot analysis for expression of CD36 in U87ΔEGFR, HDMEC, and HUVEC cells, respectively.

B: Production of secreted Vstat120 by transient transfection in 293 cells (Left). The cells (80% confluent) were left untreated (lane 1) or were transfected with either control pcDNA3.1lacZ vector (lane 2) or Vstat120 expression vector pcDNA3.1Vstat120-myc/his (lane 3). Vstat120 produced by cells transfected with full length BAI1 expression vector was utilized as a size control (lane 4). CM was collected in serum-free media for 48hrs and used in experiments B–D below. WCE, whole cell extract.

Transwell migration assays (Right) examining the migration of HUVEC and HDMEC in the presence of CM from control or Vstat120 containing CM from 293 cells. The number of cells that migrated to the bottom of the chamber after 8 hrs was quantified as described in materials and methods. Note that Vstat120 containing CM reduces the migration of HDMEC, but not HUVEC.

C. Scratch-wound migration assays. Confluent HDMECs were wounded, treated with CM prepared as in B. and the endothelial cells allowed to migrate for 8 hrs, then fixed and stained with crystal violet. Shown are representative pictures of migrated cells (Top panel). The black bars indicate initial wound width in micrometers. Distance of migration, percentage of wound closure, and speed of migration was quantified (Middle panel). The experiment was repeated twice with similar results. Data are expressed as mean +/− SEM; n=6 for each condition; * $p<0.01$ compared to Vstat120.

CD36 function-blocking antibody prevents Vstat120 anti-angiogenic function (Bottom panel). HDMECs were wounded, then either left untreated or treated with anti-CD36 function-blocking antibody at 10 μg/mL for 30 min. The cells were next treated with CM (as above) for 30 min, followed by treatment with 10% serum to induce cell migration. Final wound width was measured after 8 h and the distance migrated was calculated.

D. Transwell assay examining the migration of HBMEC in the presence of CM from U87MGD (Ctrl) and Vstat 120 expressing U14 cells (Vstat).

Data is mean ± SEM. n=3 for each condition. * $p<0.05$ and n.s. not significant by Student's T test.

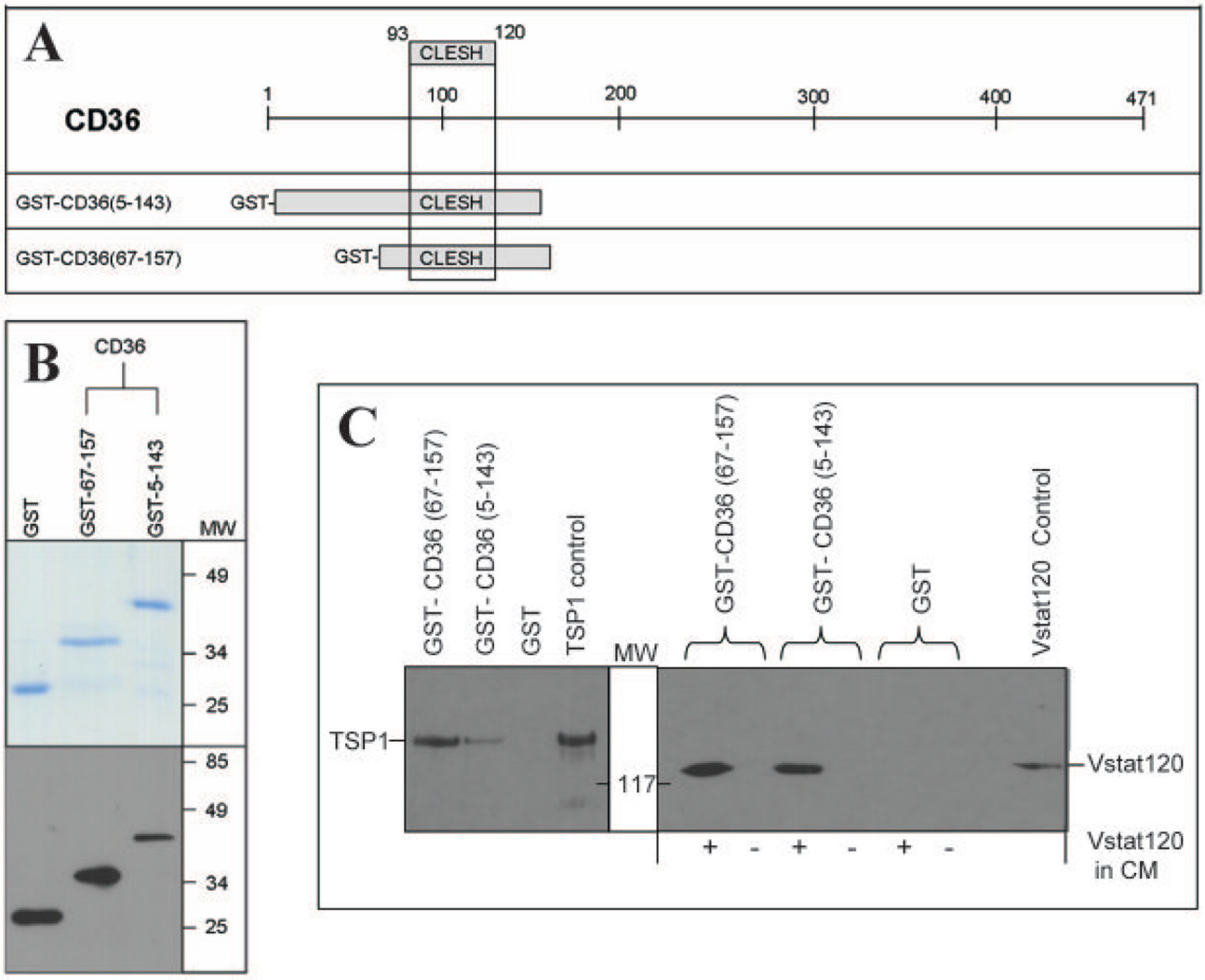

Figure 5. Vstat120 binds to the purified CLESH domain of CD36

A: Schematic of CD36 structure with the CLESH domain. The two GST-CD36 constructs used (amino acids 5–143 and 67–157), both of which contain the CLESH domain (amino acids 93–120) are shown.

B. Top: Coomassie stained gel showing purified GST, and GST tagged recombinant proteins encoding for amino acids 67–157 and 5–143 of CD36. Proteins purified to near homogeneity and migrated at their predicted molecular weight. Bottom: Western blot analysis of each fusion protein probed with anti-GST monoclonal antibody (MAB3317 Chemicon International).

C. GST pull-down assay. GST alone or the two recombinant GST-CD36 peptides were bound to glutathione sepharose beads and CM from LN229 glioma cells stably expressing Vstat120 (+ lanes) or control cells (− lanes) was tested for protein interaction. A separate pull-down assay with CM from TSP1 expressing cells (LN229 clone C9) was used as a positive control. The bound proteins were eluted and analyzed for Vstat120 and TSP1 expression by western blot. Both the GST tagged CD36 containing recombinant peptides could pull down Vstat120 and TSP1 but not the purified GST. Positive control lanes are TCA precipitations of CM (collected serum-free after 96hrs) that express either Vstat120 or TSP1.

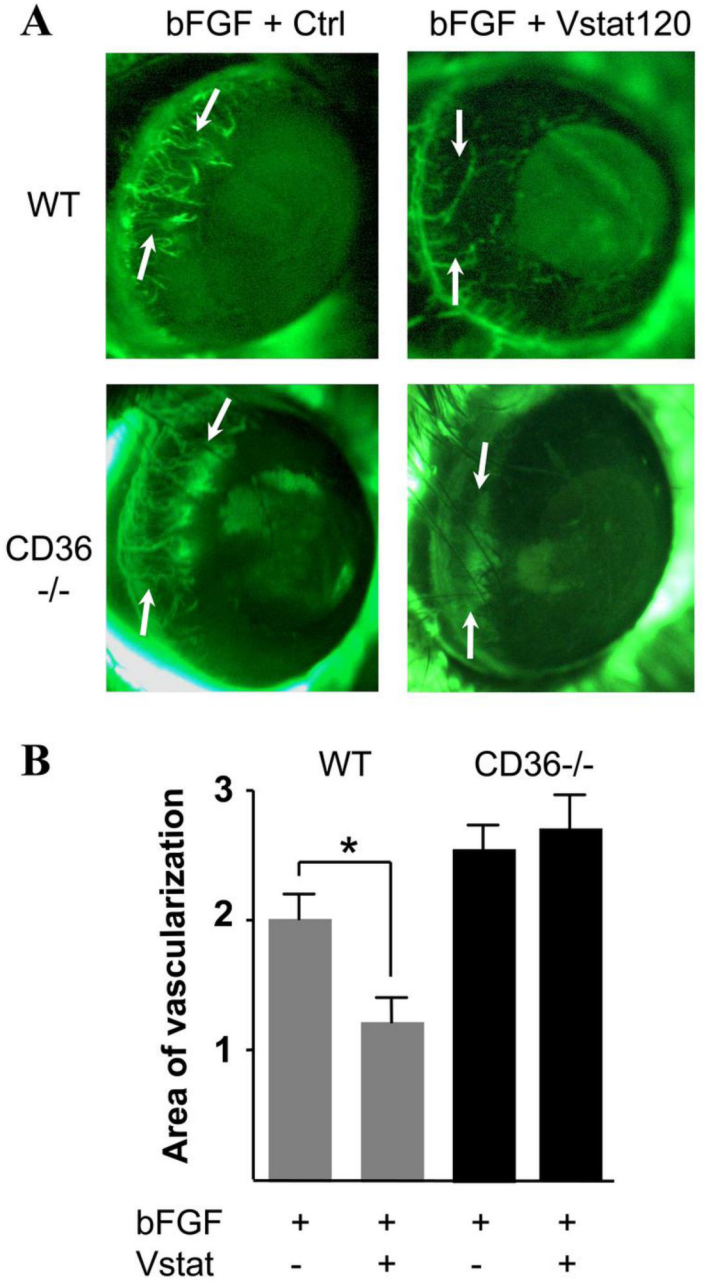

Figure 6. Vstat120 inhibits corneal angiogenesis in a CD36-dependent manner

Representative photographs (**A**) of mice cornea at 5 days post implantation of pellets containing 25ng of bFGF and CM of 293 cells (50ng total CM protein) transfected with Vstat120 or vector control (Ctrl). Photographs show FITC-dextran labeled capillaries (arrows) progressing toward the pellet, previously inserted in the mouse cornea. Angiogenic response was quantified by measuring the neovascular area in the cornea. Relative to control (**A**, upper left), CM collected from Vstat120-expressing cells (**A**, upper right) impairs capillary formation by 40%. This effect is totally negated in CD36 knockout mice (**A**, bottom pictures). The mean of neovascularized areas (mm^2) in the corneas were quantified (**B**) as described in Materials and Methods. Each

condition was carried out in at least 9 corneas. The values are expressed in means±SE. Statistical analysis was performed using the ANOVA test, *$p<0.05$.